

Gamma-ray mirror technology for NDA of spent fuel

Unclassified

September 28, 2017

M.-A. Descalle¹, J. Ruz-Armendariz¹, T. Decker¹, J. Alameda¹,
N. Brejholt¹, R. Soufli¹, J. Robinson¹, J. Dreyer¹, M.
Pivovaroff¹, K. Ziock², D. Chichester³, S. Watson³, H. Trellue⁴

¹ Lawrence Livermore National Laboratory, CA

² Oakridge National Laboratory, TN

³ Idaho National Laboratory, ID

⁴ Los Alamos National Laboratory, Los Alamos, NM



Disclaimer

This document was prepared as an account of work sponsored by an agency of the United States government. Neither the United States government nor Lawrence Livermore National Security, LLC, nor any of their employees makes any warranty, expressed or implied, or assumes any legal liability or responsibility for the accuracy, completeness, or usefulness of any information, apparatus, product, or process disclosed, or represents that its use would not infringe privately owned rights. Reference herein to any specific commercial product, process, or service by trade name, trademark, manufacturer, or otherwise does not necessarily constitute or imply its endorsement, recommendation, or favoring by the United States government or Lawrence Livermore National Security, LLC. The views and opinions of authors expressed herein do not necessarily state or reflect those of the United States government or Lawrence Livermore National Security, LLC, and shall not be used for advertising or product endorsement purposes.

Lawrence Livermore National Laboratory is operated by Lawrence Livermore National Security, LLC, for the U.S. Department of Energy, National Nuclear Security Administration under Contract DE-AC52-07NA27344.

Table of Contents

1	Introduction	5
1.1	Project goals.....	5
1.2	Future experiments	5
2	INL Benchmark experiment.....	6
3	Simulation capability for gamma mirror experiments	7
4	Three-mirror system.....	9
4.1	Simulations.....	9
4.2	Design, optimization and fabrication.....	10
4.2.1	Mirrors	10
4.2.2	Hardware	11
4.2.3	Control software	11
4.3	Testing of prototype elements	12
5	Towards focusing nested optics	15
5.1	Film deposition.....	15
5.2	Characterization	15
6	Summary	16
	References.....	17

Table of Figures

Figure 1. INL Experimental setup (left) and gamma mirror set-up (right). Red arrows indicate the path of the photons.....	6
Figure 2. Intensity map in the 57-61 keV energy range at an absolute grazing angle of 1454 arcsec. The large band on the left is an image of the direct beam and the narrow vertical band on the right corresponds to the reflected 59.54 keV Americium line (left plot). The right plot shows the rocking curve around the 59.54 keV line with data (red square) and fit (dotted blue curve)......	7
Figure 3. Ray-tracing simulation of the INL set-up at a grazing angle of 1454 arcsec.(left). Comparison of simulated intensity profile for six absolute grazing angles (colored histograms) and their summed contribution (purple) to the overall intensity profile from the INL ^{241}Am data (dashed line histogram) (right).	8
Figure 4. Ray-tracing simulation of the IFEL set-up. (left) Comparison between the intensity profiles obtained from simulation of the IFEL setup at 800 arcsec (dashed line) and the intensity profile from data (solid line) at that angle. (right)	9
Figure 5. Ray tracing simulation of the three-mirror system with narrow collimation at the exit of the IFEL port	10
Figure 6. TEM image of a thin period WC/SiC multilayer coating: dark layers are made of WC and light ones of SiC.	10
Figure 7. Rendering of the three-mirror optics with JJ-Xray slits -the real set-up include a W collimator- and alignment scope (left). Three-mirror system (right). Plates on top of mirror holder are removed during experiment.....	11
Figure 8. LabVIEW graphical user interface controlling the position and orientation of each of the three mirrors. Two modes are available: manual for alignment and automated scanning for experiments.....	12
Figure 9. Experimental set-up: the ^{133}Ba source is located in the steel cylinder on the left. A first W collimator is directly in front of cylinder and a second W collimator is in front of the mirror in the first holder. The two other holders are empty. The imaging detector on the right is aligned with the set-up so that the collimated direct beam is slightly lower than the detector centerline.....	13
Figure 10. GeGI image showing the reflected 81 keV ^{133}Ba line as a dark horizontal band at $x=10\text{mm}$. The thin horizontal band at $x=-5\text{mm}$ corresponds to the fraction of the direct beam that was not blocked and was used as a reference. The vertical bands in the center and sides are detector artifacts. Note the y-axis is the abscissa in this image.....	13
Figure 11. Total rates as a function of vertical position in the image for absolute graze angle ranging from 4600 to 5200 microrad. Each point represents the sum over a row of pixels. The direct beam is located at $x=-0.5\text{cm}$ and the reflected beam at $x=1.0\text{cm}$. Results are for a new mirror and maximum rate for the 81 KeV line was obtained at the absolute graze angle of 4971 microrad.....	14
Figure 12. Rocking curve for the 81keV ^{133}Ba line reflected on a newly coated mirror, experiment (blue square) and fit (red line).....	14
Figure 13. WC/SiC multilayer coated cylindrical glass segment in coating fixture (top right)	16
Figure 14. Measured axial (left) and radial (right) uniformity of the WC/SiC multilayer coating deposited on a thin glass 30 degree cylindrical segment.....	16

1 Introduction

Direct measurements of gamma rays emitted by fissile material have been proposed as an alternative to measurements of the gamma rays from fission products. From a safeguards applications perspective, direct detection of uranium (U) and plutonium (Pu) K-shell fluorescence emission lines and specific lines from some of their isotopes could lead to improved shipper-receiver difference or input accountability at the start of Pu reprocessing. [1,2] However, these measurements are difficult to implement when the spent fuel is in the line-of-sight of the detector, as the detector is exposed to high rates dominated by fission product emissions.

To overcome the combination of high rates and high background, grazing incidence multilayer mirrors have been proposed as a solution to selectively reflect U and Pu hard X-ray and soft gamma rays in the 90 to 420 keV energy into a high-purity germanium (HPGe) detector shielded from the direct line-of-sight of spent fuel. Several groups demonstrated that K-shell fluorescence lines of U and Pu in spent fuel could be detected with Ge detectors.[2-5] In the field of hard X-ray optics the performance of reflective multilayer coated reflective optics was demonstrated up to 645 keV at the European Synchrotron Radiation Facility.[6-8]. Initial measurements conducted at Oakridge National Laboratory with sealed sources and scoping experiments conducted at the ORNL Irradiated Fuels Examination Laboratory (IFEL) with spent nuclear fuel further demonstrated the pass-band properties of multilayer mirrors for reflecting specific emission lines into 1D and 2D HPGe detectors, respectively.[9-12].

1.1 Project goals

The goals of the project can be summarized as follows:

- Design, conduct and analyze a benchmark experiment with gamma mirrors at INL
- Develop a simulation capability for gamma mirror experiments
- Design, optimize and fabricate and test a hard x-ray measuring system to better understand background contributions observed in previous experiments
- Collect and analyze data from a measurement campaign with spent nuclear fuel.
- Investigate the feasibility of cylindrical shell multilayer coatings at LLNL for segmented X-ray and gamma ray focusing optics

Each goal is addressed in the following sections and additional details can be found in technical reports and publications. Unfortunately, the measurement campaign was not completed due to time constraints, limited availability of the experimental site (IFEL, ORNL), and unexpected additional costs incurred by the project to mitigate the loss of the ORNL imaging detector.

1.2 Future experiments

A controlled experiment at LLNL X-ray facility could be a crucial step in preparing for a deployment at IFEL; however, unlike radioactive or synchrotron light sources which deliver quasi monoenergetic photons, a bremsstrahlung beam has a broad energy spectrum which could present a challenge when trying to detect reflected X-rays within a narrow energy band if the signal to noise ratio is low. To be successful, an experiment would require a fine control of the geometrical set-up, low background, and a

well-characterized source, detector response, and background, and data that may not be available yet would then need to be measured. A scoping study will address the requirements, potential knowledge gaps and feasibility of this experiment. Finally, it is clear that the last step of the experimental demonstration of the gamma-ray mirror technology should be conducted in an appropriate facility such as the IFEL with spent nuclear fuel samples.

2 INL Benchmark experiment

The long-term goal of the LLNL gamma ray mirror program is the NDA of spent nuclear fuel to determine U and Pu content; however, previous experiments pointed to the need for stringent experimental conditions with a well-defined Pu source in a low background environment in order to evaluate the detection system characteristics.

The goal of the INL experiment was to obtain a dataset for a SNM-rich material to benchmark an end-to-end simulation suite. The experiment was conducted in INL's Zero Power Physics Reactor (ZPPR) cell in September 2014. One of the key advantages of the ZPPR cell is a low and well-documented background, and details regarding the facility can be found in the INL report.[13] K-shell fluorescence lines and gamma emission lines from a well-characterized plutonium source were reflected with a flat multilayer coated mirror into a gamma imaging germanium detector in a low background environment. The source was a legacy plutonium fuel plate with high ^{240}Pu content from the former ZPPR program. [13] A schematic of the experimental set-up and photograph of the optics are shown in Figure 1.

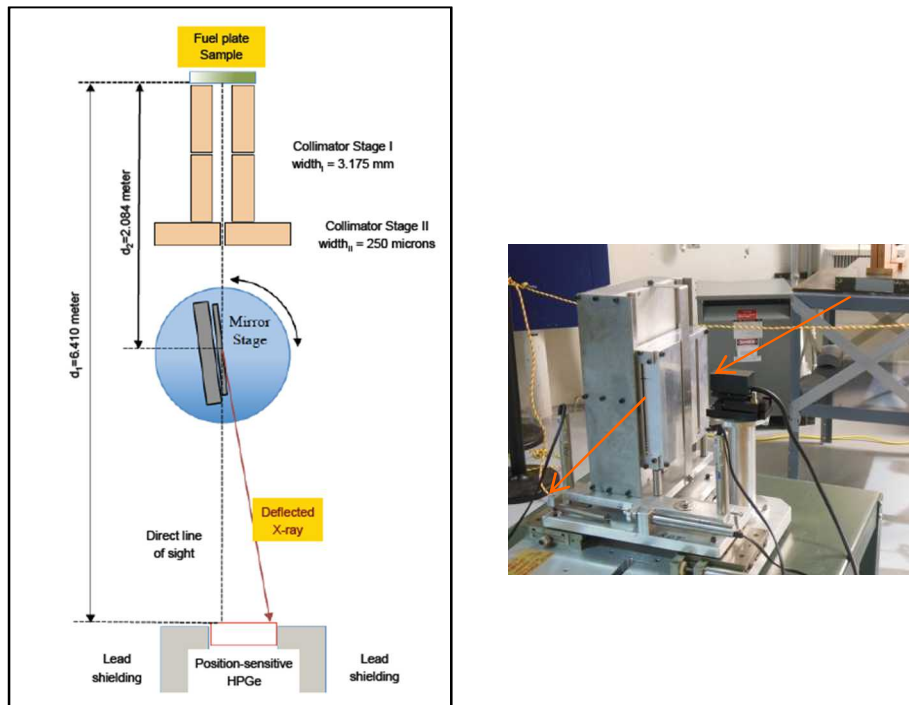


Figure 1. INL Experimental setup (left) and gamma mirror set-up (right). Red arrows indicate the path of the photons.

The X-ray mirror consisted of a single flat mirror coated with a tungsten carbide/silicon carbide (WC/SiC) multilayers made of $N=300$ bilayers with a nominal period thickness $d=15.2$ Å. The mirror has been extensively characterized at 0.8 and 8 keV and its response is well-understood up to 645 keV. The physics of multilayer optics has been described in detail in previous publications. [6-9] Gamma spectra and images were recorded with a gamma ray imaging detector or GeGI (PHDS Co., Knoxville, TN) that provides both imaging and spectral information. A complete description of the set-up and the results can be found in reference [14].

Results of the experiment are shown in Figure 2. Pu emissions in the 100 keV range were indistinguishable from background radiations; however, the 59.64 keV line of ^{241}Am was reflected off a single mirror and maximum reflectivity was demonstrated at an absolute grazing angle of 1454 arcsec corresponding to the expected Bragg angle as shown in the rocking curve in Figure 2.

In conclusion, a benchmark data set with a realistic background was obtained for the 59.64 keV line of ^{241}Am and later simulations of the plate leakage spectrum showed that the intensity of the ^{241}Am line was orders of magnitude greater than that of Pu characteristic X-rays. Similarly to previous experiments, it became clear that a simulation tool to design and optimize the experimental set-up was necessary. Several other issues were identified that informed our subsequent research: a high-precision experimental set-up between the source, optics, and detector is required for efficient data acquisition; detector non-uniformities should be minimized, and data analysis should be conducted in real-time or near real-time.

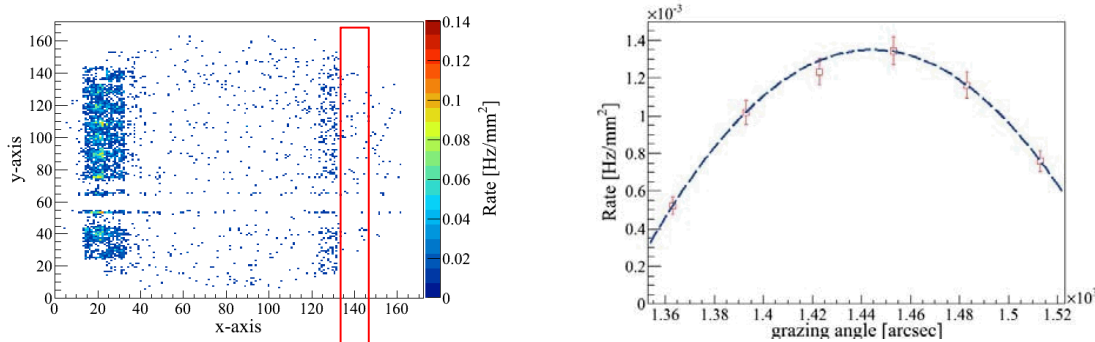


Figure 2. Intensity map in the 57-61 keV energy range at an absolute grazing angle of 1454 arcsec. The large band on the left is an image of the direct beam and the narrow vertical band on the right corresponds to the reflected 59.54 keV Americium line (left plot). The right plot shows the rocking curve around the 59.54 keV line with data (red square) and fit (dotted blue curve).

3 Simulation capability for gamma mirror experiments

The INL benchmark experiment and the earlier IFEL scoping experiment highlighted the need for predictive tools to estimate the optics response under various experimental conditions and inform the design of the final experimental set-up for direct measurements of U and Pu lines. Consequently, a simulation capability was developed based on ray-tracing that accounts for the collimation and physical layout of the experiments, the energy dependence of the multilayers and the complex spectra emitted by spent fuels or sources. A complete description can be found in reference [15] and [16].

Depending on the type of sources used in the experiment, source models can be generated with radsrv1.6 for the INL Pu fuel plate, or through a two-step process for spent fuel. For the latter model, the IFEL MOX and TMI rods are provided by H. Trellue and her team at Los Alamos National Laboratory [17] based on material composition and emission spectra obtained from burn-up calculations. Fuel pin leakage spectra can then be simulated with MCNP and used as source term for the ray-tracing step.[18]

The ray-tracing capability allows simulating the beam reflected by one or several flat mirror(s) within the experimental set-up, accounting for the mirror response or reflectivity simulated with IMD, a software commonly used to model the optical property of multilayer films.[19] The ray tracing software has several limitations: it works in 2D and for flat substrates, and background due to scatter in the experimental set-up is not accounted for. At higher photon energy, scatter should be simulated with a Monte Carlo transport code, if necessary.

This capability was validated against data from the INL and IFEL experiments and results are shown in Figure 3 and 4 respectively. [12][14] Gamma-rays from the source can either be stopped by the collimator-gate setup (yellow) or travel towards the optic (orange) and reflect onto the detector where gamma-rays reflecting at two different graze angle are shown in blue and green. The purple dashed line in the figure shows the maximum aperture of the setup, i.e gamma rays that reach the detector plane (red dashed line) with or without experiencing any reflection in the optic. In both cases, simulated intensity profiles are in good agreement with data.

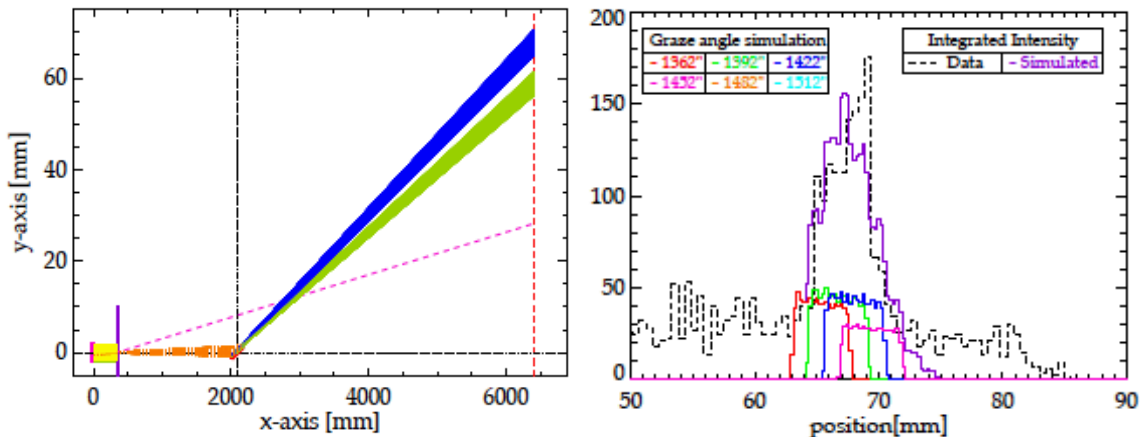


Figure 3. Ray-tracing simulation of the INL set-up at a grazing angle of 1454 arcsec.(left). Comparison of simulated intensity profile for six absolute grazing angles (colored histograms) and their summed contribution (purple) to the overall intensity profile from the INL ^{241}Am data (dashed line histogram) (right).

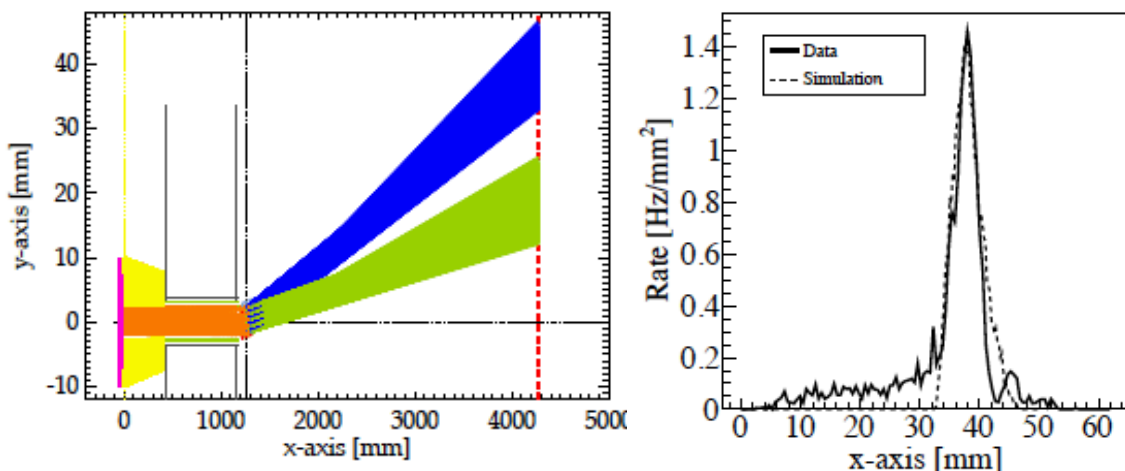


Figure 4. Ray-tracing simulation of the IFEL set-up. (left) Comparison between the simulated intensity profiles of the IFEL setup at 800 arcsec (dashed line) and the measured intensity profile (solid line) at that angle. (right)

Once validated, the simulation toolkit proved useful to both crosscheck experimental results and optimize future measurement campaigns. The ray-tracing models were modified to explore experimental configurations that could yield better signal by maximizing photon fluence: strategies ranged from reducing the source to mirror distance to reflecting X-rays on successive mirrors to better differentiate direct beam from reflected beam. The IFEL scoping measurements on spent fuel had shown significant background overall, some likely from ^{137}Cs , and detection of the Pu characteristic X-rays had proven difficult.

4 Three-mirror system

4.1 Simulations

Several alternate designs for the optics were explored to improve signal to noise ratio. Simulations showed that using a second, and possibly a third, mirror should greatly reduce the background of out-band-radiation and enhance our ability to quantify the amount of SNM present in spent nuclear fuel despite the signal loss at each reflection. Figure 5 shows simulation of optimized reflections off the proposed three-mirror system in the IFEL geometry.

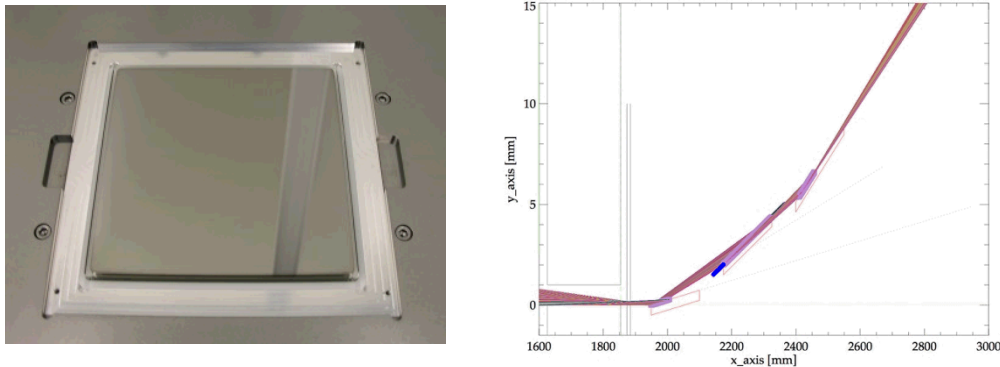


Figure 5. Ray tracing simulation of the three-mirror system with narrow collimation at the exit of the IFEL port

4.2 Design, optimization and fabrication

An additional factor may have contributed to the loss of reflectivity in the first IFEL experiment: the mirrors in the 5-mirror stack optic were made of Si wafers which in general have excellent roughness of order 1 Å rms: from the stand point of the multilayer reflectivity it is ideal, the lower the roughness of the substrate, the lower the roughness of the multilayer and the better the reflectivity. However, reflective X-ray optics rely on shallower grazing angles with increasing photon energies and the flatness of the substrate, or figure, must be considered in addition to roughness. Si wafers are thin substrates, i.e. they have limited rigidity, and they are not optimized as high-flatness substrates. Each mirror was 10 cm x 10 cm and held in an aluminum frame, a configuration that may have affected the overall figure of the optic.

4.2.1 mirrors

Taking this factor into consideration, two ultra-smooth 6" x 6" EUVL mask blanks were chosen for their demonstrated best performance in the hard X-ray and soft gamma range due to low figure error and low roughness, of order ~1 Å rms. The demonstration of a WC/SiC multilayer coating reflectivity up to 644 keV was achieved with this type of substrate. The substrates were coated with a WC/SiC multilayer made of $N=300$ bilayers with a d-spacing of 1.48 nm. A photo of one of the coated substrates and a transmission electron microscopy (TEM) of a thin multilayer are shown in Figure 6. The third mirror was the mirror used for the INL experiment and the high energy reflectance measurements.

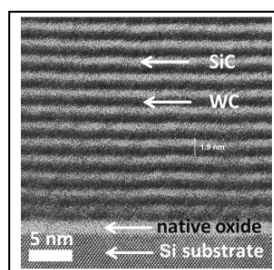


Figure 6. TEM image of a thin period WC/SiC multilayer coating: dark layers are made of WC and light ones of SiC.

4.2.2 Hardware

The multi-mirror system hardware to be deployed for the final experiment has a flexible design that enables the use of one, two, or three successive mirrors with grazing angle θ , 30, and 50. Each mirror holder is controlled by 4 actuators to set the tilt, roll, pitch and height of the mirror. The assembled mirror set up is shown in Figure 7. A 2" thick tungsten collimator is in front of the first mirror, and the height of the slit width can be adjusted as a function of grazing angle to better control the beam angular divergence. The set up allows high precision positioning of each mirror: the measured angular resolution for each mirror is better than 10 microrad.



Figure 7. Rendering of the three-mirror optics with JJ-Xray slits -the real set-up includes a W collimator- and alignment scope (left). Three-mirror system (right). Plates on top of mirror holder are removed during experiment.

4.2.3 Control software

The control software was written in LabVIEW (National instruments, Austin, TX) and can be used to perform two main tasks, mirror alignment and source sampling. The graphical user interface is shown in Figure 8. To align the mirrors, the GUI allows the user to move each actuator independently and/or to perform axial rotations for each mirror to achieve alignment with the help of a theodolite. Real time readout allows for monitoring and storing each actuator position in an ascii file. The frequency of the plotting routine and data writing can be adjusted by the user in the GUI to check the proper movement of each actuator and to control the size of the storage data file if necessary.

To scan a source emission spectrum, the software has a sequential routine that can be switched on/off by the user in the GUI. The scan routine allows the user to position the mirrors at a given low grazing angle (high energy value) and ramp up to a final grazing angle (lower energy value) with a user specified number of steps and dwell time. The automated routine can be used as a standalone method or in conjunction with a detector. An RS232 communication protocol has been established such that the automated routine can synchronize with a given detector.

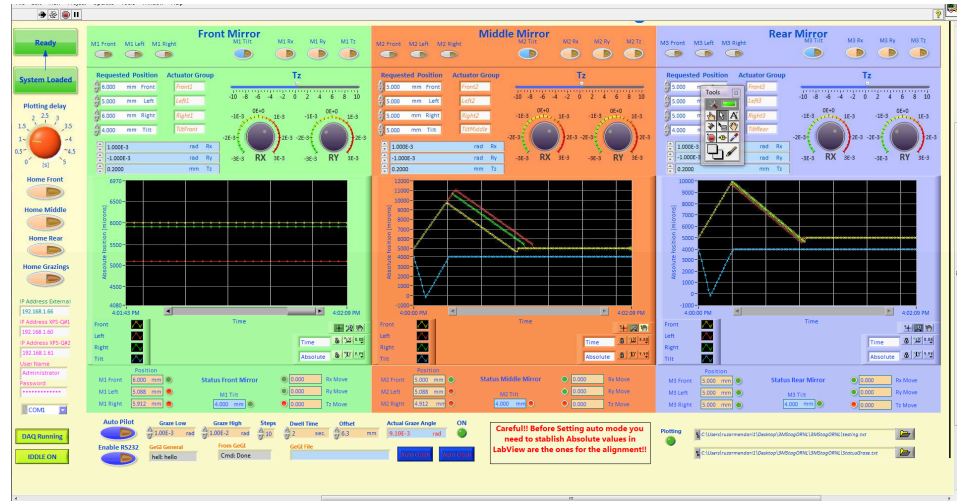


Figure 8. LabVIEW graphical user interface controlling the position and orientation of each of the three mirrors. Two modes are available: manual for alignment and automated scanning for experiments.

4.3 Testing of prototype elements

The purpose of this experiment was to test the complex alignment protocol between mirrors, collimators, and source, to check the response of the new mirrors, and to achieve two reflections in order to check the location of the reflected signal against simulations.

The three mirrors were characterized individually with the experimental set-up shown in Figure 9. A 0.788 mCi ^{133}Ba source was chosen for its 81 keV emission line close to the range of U and Pu characteristic X-rays. The source was 0.7 cm in diameter and was placed in a bore at the center of a steel cylinder doubling as a small collimator and shielding. Two tungsten (W) collimators with slit height of 750 micron were located next to the steel shield and in front of the first mirror holder, respectively. The ORNL GeGI detector was unavailable due to technical issues, and a newer LLNL GeGI 4S from Morgan Burks' group was used. Consequently, new communication protocol and software were developed in collaboration with Jonathan Dreyer to enable data acquisition automation with feedback loop to start data acquisition following each angular step.

The GeGI was aligned with the three-mirror set-up and the source so that the top of the collimated direct beam would be at $x=-0.5$ cm below the center of the image. Once set, the detector line-of-sight of the direct beam was blocked with copper blocks, with the exception of a narrow band of a few pixels used as a reference during $\theta/2\theta$ reflectivity measurements which appears as the bottom dark strip on the image shown in Figure 10. The mirror was rotated from 4600 to 5200 microrad in 60 microrad increment with 5 hours of dwell time at each position. Images such as the one shown in Figure 10 were acquired at each angle. Counts were summed along pixel rows and results are plotted for a series of angles in Figure 11. Finally, the rocking curve of the mirror at 81 keV in Figure 12 shows rate in the reflected peak as a function of angle. The peak reflectivity is at a grazing angle of 4950 microrad for the fit while the calculated Bragg angle for a d-spacing of 1.48 nm at 81 keV is 5172 microrad. The difference is likely due to the source divergence and a small misalignment.

For the final experiment, two mirrors were placed in the holders closest to the collimator to reflect the beam twice. We did not detect signal above background at the expected position in the image, despite the ray-tracing simulations and estimations from the one-reflection results. The ray tracing simulations may

be overestimating the reflected signal since it does not take into account the lateral divergence of the beam incident on the first mirror or the reflected beams.

Despite not being able to observe a second reflection under the experimental conditions reported here, these tests were successful in demonstrating the reflectivity of the newly coated mirrors at 81 keV, the robustness of automation and of the communication protocol, and the accuracy of the mirror positioning. It also highlighted the complexity and time required to align the system properly.

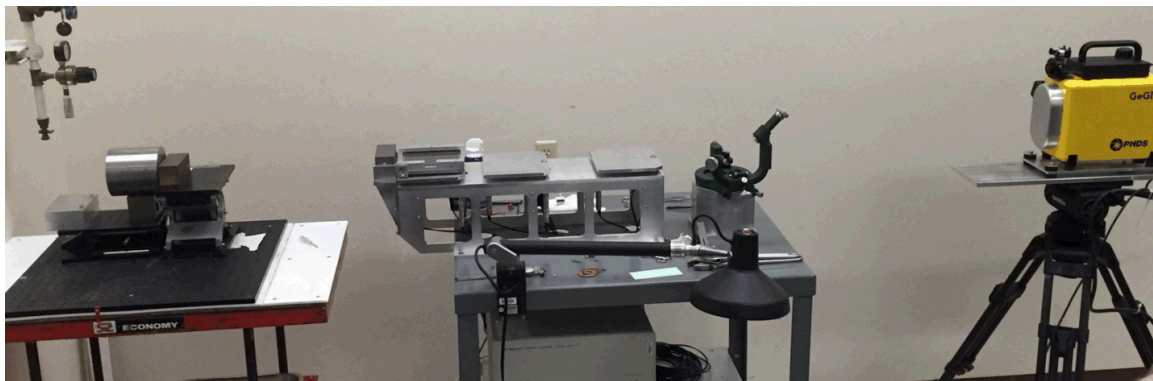


Figure 9. Experimental set-up: the ^{133}Ba source is located in the steel cylinder on the left. A first W collimator is directly in front of cylinder and a second W collimator is in front of the mirror in the first holder. The two other holders are empty in this picture. The imaging detector on the right is aligned with the set-up so that the collimated direct beam is slightly lower than the detector centerline.

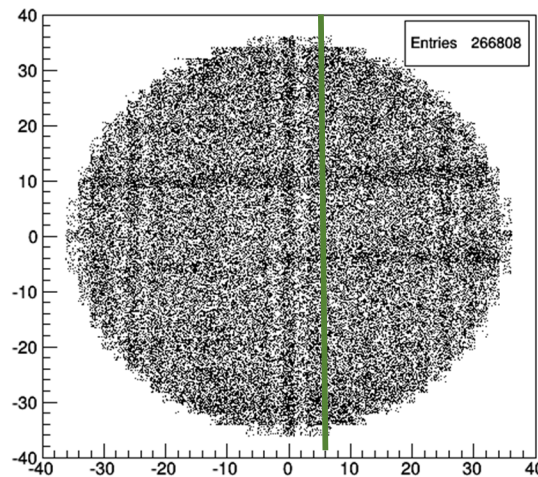


Figure 10. GeGI image showing the reflected 81 keV ^{133}Ba line as a dark horizontal band at $x=10\text{mm}$. The thin horizontal band at $x=-5\text{mm}$ corresponds to the fraction of the direct beam that was not blocked and was used as a reference. The vertical bands in the center and sides are detector artifacts. Note the y-axis is the abscissa in this image.

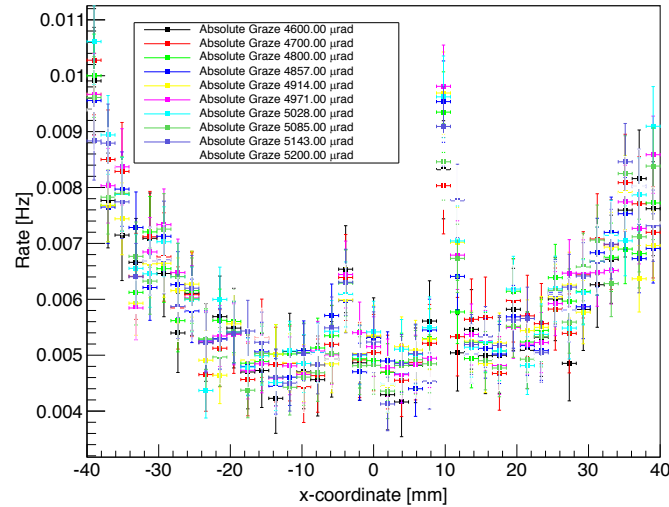


Figure 11. Total rates as a function of vertical position in the image (green line in figure 10) for absolute graze angle ranging from 4600 to 5200 microrad. Each point represents the sum over a row of pixels. The direct beam is located at $x=-0.5$ cm and the reflected beam at $x=1.0$ cm. Results are for a new mirror and maximum rate for the 81 keV line was obtained at the absolute graze angle of 4971 microrad.

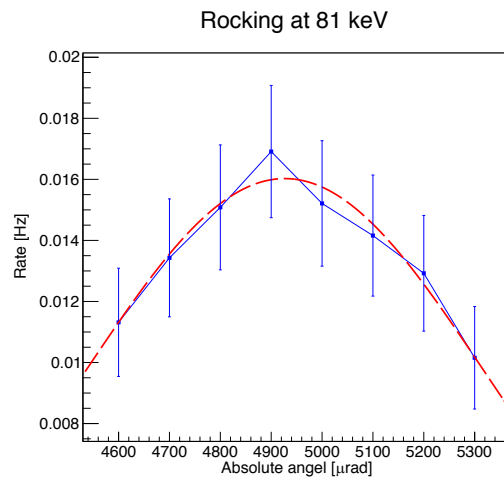


Figure 12. Rocking curve for the 81 keV ^{133}Ba line reflected on a newly coated mirror, experiment (blue square) and fit (red line).

5 Towards focusing nested optics

Experiments conducted by our team so far have relied on single bounce off a flat substrate that can only result in a small solid angle at the detector. In the context of safeguards, focusing nested optics based on Wolter I design such as those developed by the Astrophysics community for the last decades would 1) enable focusing of the signal through two bounces into a smaller detector located at or near the focal plane and 2) and with a nested configuration, greatly increase photon collection efficiency by increasing the solid angle by several order of magnitude at the detector depending on the number of layers. General background and background due to 662 keV photons are expected to be reduced thus improving signal-to-noise ratio. However, several issues need to be addressed when considering segmented focusing optics for hard X-rays and soft gamma rays in the 100 keV range and above, namely requirements on film uniformity along the cylindrical segment axis and radii and on the substrate roughness and figure.

5.1 Film deposition

LLNL magnetron sputtering systems were designed to coat planar or quasi-planar substrates. The deposition model for these systems was modified and validated to enable coating of cylindrical segments with greater curvature such as those used to build segmented focusing optics. It was determined that uniformity should be better than 1% or better axially and under 3.5% radially to achieve a $\Delta\theta$ of 30 arcsec at 100 keV and with a d-spacing of 1.5 nm. A multidimensional parametric search helped determine initial deposition parameters and a multilayer coating was deposited on a 30 degree cylindrical shell segment made of NuSTAR glass, i.e. 210 micron thick Schott glass, with a radius of 7.8 cm and a length of 22.5 cm. It consisted of N=150 bilayers of WC/SiC with a d-spacing of 1.48 nm. Figure 13 shows the coated cylindrical sample in its aluminum fixture.

5.2 Characterization

Measurements of the uniformity and reflectance of the multilayer coating were conducted at the calibration and standards beamline 6.3.2 at the Advanced Light Source (ALS) at a beam incidence angle of 80 degrees. Reflectances for a range of wavelengths between 2.5 and 2.65 nm were of order 1.5e-4 to 1.2e-3 or several orders of magnitude lower than expected. At least three factors have been identified that may contribute to the low peak reflectivity: the roughness of the substrate, the incidence angle of the measurements, and the coating process. First, the roughness of the NuSTAR Schott glass sample that we coated was not available and should be measured since published data for the NuSTAR glass are sparse and vary by almost a factor of 2, from 2.0 to 3.8 Å, this is at best twice that of ultra-smooth mask blanks. Second, to ensure sufficient beam intensity, the beam incidence on the sample was set to 80 degrees or near normal incidence, which can yield reflectivities lower by 1 to 2 orders of magnitude. Finally, it is expected that additional iterations are necessary to understand possible geometric effects during coating and optimize the deposition process.

Measurements of the axial and radial multilayer thickness are plotted in Figure 14. Uniformity along the central axis of the optic was 0.5% peak to valley, better than the 1% prescription. The radial uniformity measured at axial position of 4 mm and 54 mm respectively was 6 and 5.8% peak-to-valley thickness variations, higher than our requirements of 3.5%. However, this first result is extremely encouraging and it is anticipated that the uniformity requirements would be met after further optimization of the deposition model.



Figure 13. WC/SiC multilayer coated cylindrical glass segment in coating fixture

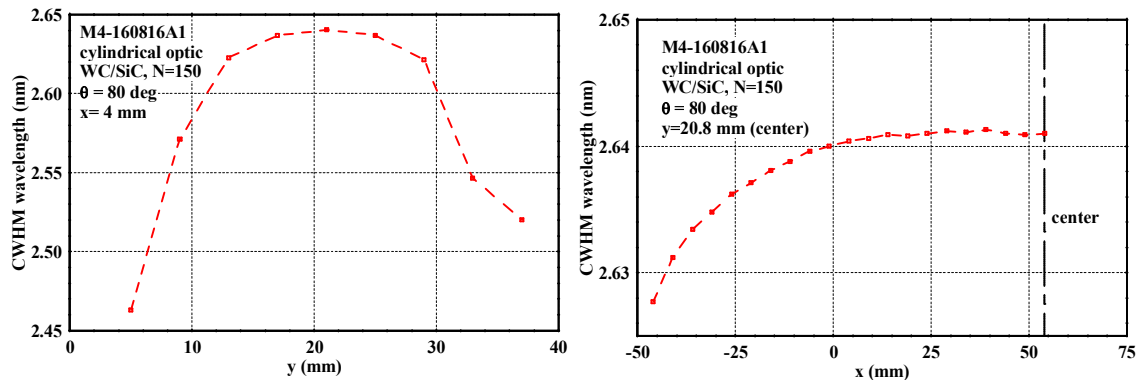


Figure 14. Measured axial (left) and radial (right) uniformity of the WC/SiC multilayer coating deposited on a thin glass 30 degree cylindrical segment.

6 Summary

The gamma mirror technology relies on developments in hard x-ray reflective optics and WC/SiC multilayer coatings. It has been advanced in the laboratory on several fronts to address low signal-to-noise ratio gain observed in previous experiments possibly due to the small deflection angle after a single reflection, an intense shallow angle scatter of 662 keV photons from ^{137}Cs in SNF, and substrate figure. A benchmark data set for the ^{241}Am 59.64 keV line was obtained during a experiment conducted at INL ZPPR facility using a fresh Pu fuel plate. A simulation capability was developed and validated with the Am 241 data and the IFEL measurements and was then used to investigate possible design of two or three bounce systems that could lower background contributions. A three-mirror system was designed, optimized, fabricated. The optic and GeGI system was tested in the lab in preparation for an experimental campaign. As a first step towards the development of nested focusing optics, initial results of cylindrical substrate coating with WC/SiC multilayers in a linear magnetron sputtering tool indicate that excellent axial uniformity of less than 1% and a radial uniformity of ~6% higher. While improvement in multilayer uniformity is still needed, other issues are fairly well understood, and nested focusing optics relying on two reflections are a promising solution to providing the much needed improvement in signal by an order of magnitude or more while reducing the impact of high background.

In addition to providing updates via quarterly reports and annual presentations at the WMS meetings, the team presented results at an international conference (IEEE NSS/MIC 2016), workshops, compiled results in technical reports and published results in a peer-reviewed journal.

- D. L. Chichester, "Properties of nuclear fuel used in tests with the LLNL gamma ray mirror in September 2014", INL/MIS-14-33068 (2014).
- J. Ruz, N. Brejnholt, T. Decker, R. Hill, M.-A. Descalle, M. J. Pivovaroff, K. P. Ziock, D. L. Chichester and S. M. Watson, "Gamma ray mirror experimental campaign at INL's ZPPR facility: Preliminary report," LLNL-TR-666071 (2015).
- M.-A. Descalle, J. Ruz, M. J. Pivovaroff, K. Ziock and H. Trellue, "New simulation capability for gamma rays mirror experiments," LLNL-TR-677932 (2015).
- J. Ruz, M.-A. Descalle, J. Alameda, N. Brejnholt, D. L. Chichester, T. A. Decker, M. Fernandez-Perea, R. M. Hill, R. A. Kisner, A. M. Melin, B. W. Patton, R. Soufli, H. Trellue, S. M. Watson, K. P. Ziock and M. J. Pivovaroff, "Characterization and simulation of soft gamma ray mirrors for their use with spent fuel rods at reprocessing facilities," Appl. Opt. 55, 16, 4285-4292 (2016).

We gave briefings on the gamma mirror technology to the IAEA technology foresight specialist and to a South Korean delegation made of representatives of the Nuclear Security and Safety Commission, the Korean Institute for Nuclear Non-proliferation and Control and the Korea Atomic Energy Research Institute during the 19th U.S. ROK permanent coordinating group meeting at LLNL.

Finally, RXO, LLC - a company we collaborate with that specialized in multilayer film deposition- submitted a Phase 1 DOE SBIR related to multilayer coatings for hard X-rays optics for Safeguards applications; it received favorable reviews but did not get funded.

References

1. T. Hayakawa, et al., Nuclear Instruments and Methods A 621 695(2010).
2. A.S. Stafford, "Spent Nuclear Fuel Self-Induced XRF to Predict Pu to U Content," M.S. Thesis, Nuclear Engineering Texas A&M University, College Station, TX (August 2010)s.
3. A.V. Bushuev, et al., Atomic Energy 53 (1982).
4. C. Rudy, P. Staples, K. Serednuik, and I. Yakovlev , "Determination of Pu in spent fuel assemblies by X-ray fluorescence," Proceedings of 46th Annual Meeting of the INMM, (2005).
5. W. S. Charlton et al. The use of self-induced XRF to quantify the Pu content in PWR spent nuclear fuel, Proceedings of the 31st Annual Meeting of ESARDA, (2009).
6. M. Fernandez-Perea, M. J. Pivovaroff, R. Soufli, J. Alameda, P. Mirkarimi, M.-A. Descalle, S. L. Baker, T. McCarville, K. P. Ziock, D. Hornback, S. Romaine, R. Bruni, Z. Zhong, V. Honkimaki, E. Ziegler, F. E. Christensen and A. C. Jakobsen, "Ultra-short-period WC/SiC multilayer coatings for x-ray applications," Nucl. Instrum. Meth A, 710:114 (2013).
7. M. Fernandez-Perea, M.-A. Descalle, R. Soufli, K. P. Ziock, J. Alameda, S. L. Baker, T. J. McCarville, V. Honkimaki, E. Ziegler, A. C. Jakobsen, F. E. Christensen and M. J. Pivovaroff, "Physics of reflective optics for the soft gamma-ray photon energy range," Phys. Rev. Let. 111:027404 (2013).
8. N. Brejnholt, R. Soufli, M.-A. Descalle, M. Fernandez-Perea, F. Christensen, A. Jakobsen, V. Honkimaki, M. J. Pivovaroff, "Demonstration of multilayer reflective optics at photon energies above 0.6 MeV," Opt. Exp., 22, 15364-15369, (2014).
9. M. J. Pivovaroff, K. P. Ziock, M. Fernandez-Perea, M. J. Harrison and R. Soufli, "Gamma-ray mirrors for direct measurement of spent nuclear fuel," Nucl. Instrum. Meth. A, 743 109–113 (2014).
10. K. P. Ziock, J. Alameda, N. Brejnholt, T. Decker, M.-A. Descalle, M. Fernandez-Perea, R. Hill,

R. Kisner, M. Melin, B. Patton, J. Ruz, R. Soufli and M. J. Pivovaroff, "U and Pu Gamma-Ray Measurements of Spent Fuel Using a Gamma-Ray Mirror Band-Pass Filter," Proceedings of Symposium on International Safeguards: Linking Strategy, Implementation and People. 20-24 October 2014, Vienna Austria. (Oct 2014).

11. M. J. Pivovaroff, K. P. Ziock, J. Alameda, N. Brejnholt, T. Decker, M.-A. Descalle, M. Fernandez-Perea, R. Hill, R. Kisner, M. Melin, B. Patton, J. Ruz and R. Soufli, "Direct Measurement of U-235 and Pu-239 in Spent Fuel Rods with Gamma-Ray Mirrors, LLNL-TR-671925, (2015).
12. J. Ruz, N. Brejnholt, J. Alameda, T. Decker, M.-A. Descalle, M. Fernandez-Perea, R. Hill, R. Kisner, M. Melin, B. Patton, J. Ruz, R. Soufli and M. J. Pivovaroff, "Direct measurement of U-235 in spent fuel rods with Gamma-ray mirrors", Nucl. Instrum. Meth. A, 777, 15-19, (2015)
13. D. L. Chichester, "Properties of nuclear fuel used in tests with the LLNL gamma ray mirror in September 2014," INL/MIS-14-33068 (2014).
14. J. Ruz, N. Brejnholt, T. Decker, R. Hill, M.-A. Descalle, M. J. Pivovaroff, K. P. Ziock, D. L. Chichester and S. M. Watson, "Gamma ray mirror experimental campaign at INL's ZPPR facility: Preliminary report," LLNL-TR-666071 (2015).
15. M.-A. Descalle, J. Ruz, M. J. Pivovaroff, K. Ziock and H. Trellue, "New simulation capability for gamma rays mirror experiments," LLNL-TR-677932 (2015).
16. J. Ruz, M.-A. Descalle, J. Alameda, N. Brejnholt, D. L. Chichester, T. A. Decker, M. Fernandez-Perea, R. M. Hill, R. A. Kisner, A. M. Melin, B. W. Patton, R. Soufli, H. Trellue, S. M. Watson, K. P. Ziock and M. J. Pivovaroff, "Characterization and simulation of soft gamma ray mirrors for their use with spent fuel rods at reprocessing facilities," Appl. Opt. 55, 16, 4285-4292 (2016).
17. Initial MCNP6 Release Overview, MCNP6 Beta 2. Los Alamos National Laboratory Report No. LA-UR-11-07082 (2011).
18. L. Hiller, T. Gosnell, J. Gronberg, D. Wright, "Radsrc Library and Application manual," UCRL-TM-229497 (2013).
19. D. Windt, IMD, Computers in Physics, 12, 360 (1998).